Fingerprint-Based Fuzzy Vault: Implementation and Performance

Article *in* IEEE Transactions on Information Forensics and Security · January 2008

DOI: 10.1109/TIFS.2007.908165 · Source: IEEE Xplore

CITATIONS
474

READS
993

3 authors, including:

Karthik Nandakumar
Institute for Infocomm Research
32 PUBLICATIONS **6,414** CITATIONS

SEE PROFILE

S. Pankanti
IBM
284 PUBLICATIONS **14,187** CITATIONS

SEE PROFILE

Fingerprint-based Fuzzy Vault: Implementation and Performance

Karthik Nandakumar, *Student Member, IEEE,* Anil K. Jain, *Fellow, IEEE* and Sharath Pankanti, *Senior Member, IEEE*

Abstract

Reliable information security mechanisms are required to combat the rising magnitude of identity theft in our society. While cryptography is a powerful tool to achieve information security, one of the main challenges in cryptosystems is to maintain the secrecy of the cryptographic keys. Though biometric authentication can be used to ensure that only the legitimate user has access to the secret keys, a biometric system itself is vulnerable to a number of threats. A critical issue in biometric systems is protecting the template of a user which is typically stored in a database or a smart card. The fuzzy vault construct is a biometric cryptosystem that secures both the secret key and the biometric template by binding them within a cryptographic framework. We present a fully automatic implementation of the fuzzy vault scheme based on fingerprint minutiae. Since the fuzzy vault stores only a transformed version of the template, aligning the query fingerprint with the template is a challenging task. We extract high curvature points derived from the fingerprint orientation field and use them as helper data to align the template and query minutiae. The helper data itself does not leak any information about the minutiae template, yet contains sufficient information to align the template and query fingerprints accurately. Further, we apply a minutiae matcher during decoding to account for non-linear distortion and this leads to significant improvement in the genuine accept rate. We demonstrate the performance of the vault implementation on two different fingerprint databases. We also show that performance improvement can be achieved by using multiple fingerprint impressions during enrollment and verification.

This research was supported by Army Research Office contract W911NF-06-1-0418.

Index Terms

Biometric cryptosystems, fuzzy vault, polynomial reconstruction, minutiae, fingerprint alignment, helper data, minutiae mosaicing

I. INTRODUCTION

Cryptographic techniques are being widely used for ensuring the secrecy and authenticity of information [1]. Although several cryptosystems have proven security guarantees (e.g., AES and RSA), the security relies on the assumption that the cryptographic keys are known only to the legitimate user. Maintaining the secrecy of keys is one of the main challenges in practical cryptosystems. The keys are usually stored in a secure location (e.g., tamper-resistant hardware) and password-based authentication is commonly used for controlling access to cryptographic keys [2]. However, passwords can be easily lost, stolen, forgotten or guessed using social engineering [3] and dictionary attacks. Limitations of password-based authentication can be alleviated by using stronger authentication schemes such as biometrics. Biometric systems [4] establish the identity of a person based on her anatomical or behavioral traits such as face, fingerprint, iris, voice, etc. Biometric authentication is more reliable than password-based authentication because biometric traits cannot be lost or forgotten and it is difficult to share or forge these traits. Hence, biometric systems offer a natural and reliable solution to the problem of user authentication in cryptosystems.

Biometric cryptosystems can operate in one of the following three modes, (i) key release, (ii) key binding and (iii) key generation. In the *key release mode*, biometric authentication is completely decoupled from the key release mechanism. The biometric template and the key are stored as separate entities and the key is released only if the biometric matching is successful. In the *key binding mode*, the key and the template are monolithically bound within a cryptographic framework (see Figure 1). It is computationally infeasible to decode the key or the template without any knowledge of the user's biometric data. A crypto-

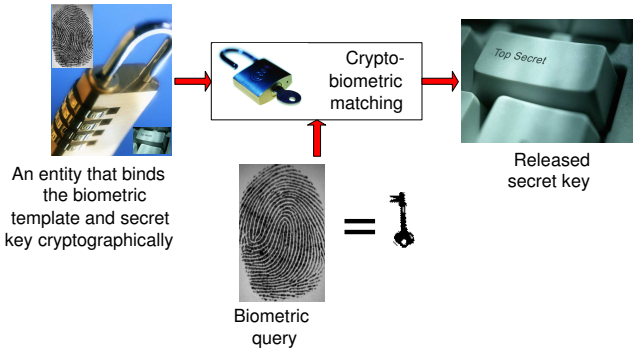

Fig. 1. Operation of a biometric cryptosystem in the key binding mode.

biometric matching algorithm is used to perform authentication and key release in a single step. In the *key generation mode*, the key is derived directly from the biometric data and is not stored in the database.

Though it is easy to implement a biometric cryptosystem in the key release mode, such a system is not appropriate for high security applications because it has two major vulnerabilities. Firstly, the biometric template is not secure. Template security is a critical issue in biometric systems because stolen templates cannot be revoked. Secondly, since authentication and key release are decoupled, it is possible to override the biometric matcher using a Trojan horse program [5]. Biometric cryptosystems that work in the key binding/generation modes are more secure but difficult to implement due to large intra-class variations in biometric data, i.e., samples of the same biometric trait of a user obtained over a period of time can differ substantially. For example, factors such as translation, rotation, non-linear distortion, skin conditions and noise lead to intra-class variations in fingerprints [6] (see Figure 2).

Juels and Sudan [7] proposed a cryptographic construction called *fuzzy vault* that operates in the key binding mode and, in principle, can compensate for intra-class variations in the biometric data. We present a fully automatic implementation of the fuzzy vault scheme based on fingerprint minutiae. Since the fuzzy vault scheme stores only a transformed version of the template, the main implementation challenge is the alignment (registration) of query fingerprint to the original template. In our implementation, we store high curvature points derived from the orientation field of the template fingerprint as helper data to assist

Fig. 2. Illustration of intra-class variability in fingerprints. Two different impressions of the same finger obtained on different days are shown with minutia points marked on them. Due to translation, rotation and distortion, the number and location of minutiae in the two images are different. The number of minutiae in the left and right images is 33 and 26, respectively. The number of common minutiae in the two images is 16 and few of these correspondences have been indicated in the figure.

in alignment. The helper data accurately aligns the template and query minutiae but does not reveal any information about the minutia points that form the template.

The rest of the paper is organized as follows. Section II introduces the basic fuzzy vault construction and section III gives the details of the proposed fuzzy vault implementation using fingerprint minutiae. The automatic fingerprint alignment technique based on helper data is described in section IV. The experimental results are presented in section V and section VI presents a discussion on the security of the system. Section VII summarizes our work and provides pointers for future research.

II. Background

Several schemes have been proposed in the literature for implementing a biometric cryptosystem in key binding/generation modes [8]–[13]. It is also worth mentioning that the problem of key binding/generation in a biometric cryptosystem is closely related to other research issues in biometrics such as template protection [14], [15] and generation of cancelable templates [16]. A detailed review of different biometric

cryptosystems has been presented in [17]. Based on this study, it is clear that the techniques proposed in [8]–[15] have their own advantages and limitations in terms of security, computational cost, storage requirements, applicability to different kinds of biometric representations and ability to handle intra-class variations in biometric data. In this paper, we focus on a specific algorithm known as fuzzy vault which was originally proposed by Juels and Sudan in [7].

A. Fuzzy Vault

Fuzzy vault [7] is a cryptographic construction that is designed to work with biometric features which are represented as an *unordered set* (e.g., minutiae in fingerprints). The security of the fuzzy vault scheme is based on the infeasibility of the *polynomial reconstruction problem*, which is a special case of the Reed-Solomon list decoding problem. The ability to deal with intra-class variations in the biometric data along with its ability to work with unordered sets which is commonly encountered in biometrics, makes the fuzzy vault scheme a promising solution for biometric cryptosystems.

Figure 3 depicts the operation of a fuzzy vault scheme. Suppose that a user wishes to hide a secret K (e.g., a cryptographic key) using his biometric sample (template) which is represented as an unordered set X. The user selects a polynomial $\mathcal{P}$ that encodes the secret K and evaluates the polynomial on all elements in X. The user then chooses a large number of random chaff points which do not lie on the polynomial $\mathcal{P}$. The entire collection of points consisting of both points lying on $\mathcal{P}$ and those that do not lie on $\mathcal{P}$ constitute the vault V. The chaff points conceal the genuine points lying on $\mathcal{P}$ from an attacker. Since the points lying on $\mathcal{P}$ encode the complete information about the template X and the secret K, concealing these points secures both the template and the secret simultaneously.

The user can retrieve the secret K from the vault V by providing another biometric sample (query). Let the query be represented as another unordered set X'. If X' overlaps substantially with X, then the user can identify many points in V that lie on $\mathcal{P}$. If sufficient number of points on $\mathcal{P}$ can be identified,

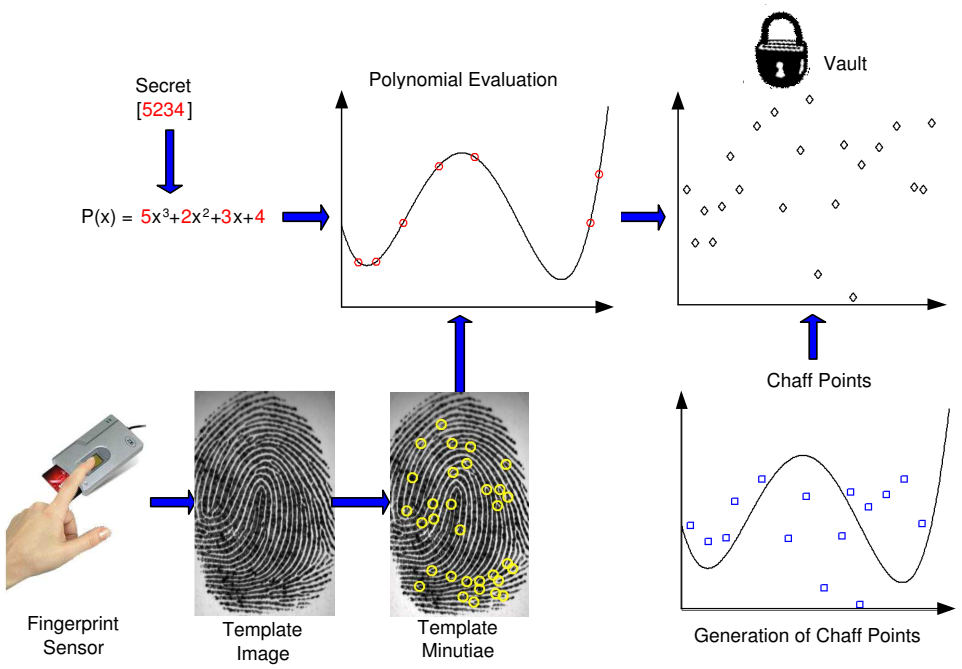

(a)

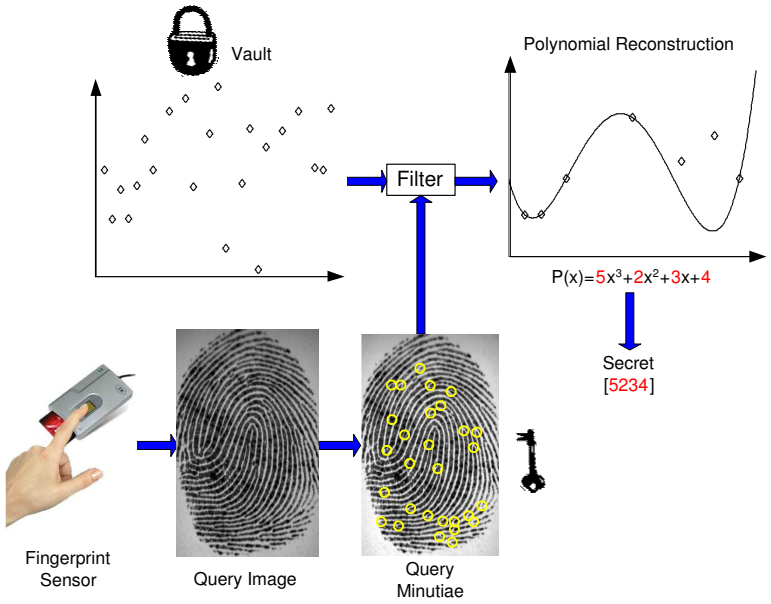

(b)

Fig. 3. Operation of the fuzzy vault scheme in [7] based on fingerprint minutiae. (a) Vault encoding and (b) vault decoding.

an error correction scheme can be applied to exactly reconstruct $\mathcal{P}$ and thereby decode the secret K. If $X^{'}$ does not overlap substantially with X, it is infeasible to reconstruct $\mathcal{P}$ and the authentication is unsuccessful. Since the secret can be retrieved from the vault even when X and $X^{'}$ are not exactly the same, this scheme is referred to as a *fuzzy* vault.

The three main parameters in the fuzzy vault scheme are r, s and n. The parameter r denotes the number of points in the vault that lie on the polynomial $\mathcal{P}$ and it depends on the number of features that can be extracted from the template (e.g., number of minutia points in the user's fingerprint). The parameter s represents the number of chaff points that are added and this parameter influences the security of the vault. If no chaff points are added, the vault reveals the information about the template and the secret. As more chaff points are added, the security increases. Typically, the number of chaff points is an order of magnitude larger than the number of genuine points ($s \gg r$). Parameter n denotes the degree of the encoding polynomial and it controls the tolerance of the system to errors in the biometric data.

In order to retrieve the secret from the vault V, the user selects a subset of r points from V which known as the unlocking set. Unlocking set is selected based on the query $X^{'}$. A (r, n) Reed-Solomon decoding algorithm [18] is then applied to search for a polynomial $\mathcal{P}$ of degree n such that more than $\frac{r+n}{2}$ points[1] in the unlocking set lie on $\mathcal{P}$. If the number of discrepancies in the biometric data $\left(|X - X^{'}|\right)$ is less than $\frac{r-n}{2}$ a valid polynomial $\mathcal{P}$ can be found and the secret K can be successfully retrieved.

B. Fuzzy Vault Implementation

Since the introduction of the fuzzy vault scheme, several researchers have attempted to implement it in practice. Clancy et al. [19] proposed a fuzzy vault scheme based on the location of minutia points in a fingerprint. They assumed that the template and query minutiae sets are pre-aligned, which is not a realistic assumption in practice. Further, four fingerprint impressions of a user were used during enrollment for

[1]The Berlekamp-Walsh algorithm [18] for Reed-Solomon list decoding can correct up to e errors only if $(n + 2e) < r$.

identifying the reliable minutia points and the error correction step was simulated without being actually implemented. The False Reject Rate[2] of their system was 20-30% and they claimed that retrieving the secret was 2^{69} times more difficult for an attacker than for a genuine user.

The fingerprint-based fuzzy vault proposed by Yang et al. [20] also used only the location information about the minutia points. Four impressions were used during enrollment to identify a reference minutia and the relative position of the remaining minutia points with respect to the reference minutia was represented in the polar coordinate system. This scheme was evaluated on a small database of 10 fingers and a FRR of 17% was reported. Chung et al. [21] proposed a geometric hashing technique to perform alignment in a minutiae-based fingerprint fuzzy vault. Fuzzy vault implementations based on other biometric modalities such as face [22] and handwritten signature [23] have also been proposed.

Uludag et al. [24] introduced a modification to the fuzzy vault scheme, which eliminated the need for Reed-Solomon polynomial decoding. They also proposed the use of helper data to automatically align the template and query minutiae sets [25]. Our fuzzy vault implementation extends the ideas presented in [24] and [25] in order to achieve a better recognition performance.

III. Proposed Fuzzy Vault Implementation

The proposed fuzzy vault implementation is based on minutiae which are local ridge characteristics (endings and bifurcations) in a fingerprint. We use both the location and orientation attributes of a minutia point in our implementation. These attributes are represented as a 3-tuple (u, v, θ), where u and v indicate the row and column indices in the image, and θ represents the orientation of the minutia with respect to the horizontal axis ($1 \leq \theta \leq 360$). The algorithm described in [26] is used for minutiae extraction.

We have implemented the modified fuzzy vault construction proposed in [24]. This modified fuzzy vault scheme does not require Reed-Solomon decoding. Instead, several candidate sets of size $(n + 1)$

[2]False Reject Rate (FRR) refers to the percentage of attempts in which the authentication is unsuccessful for a genuine user.

(where n is the degree of the polynomial which encodes the secret) are generated from the unlocking set and polynomials are reconstructed using Lagrange interpolation. This method gives rise to several candidate secrets and Cyclic Redundancy Check (CRC) based error detection technique is used to identify the correct polynomial and hence decode the correct secret. The advantage of this scheme is its increased tolerance to biometric intra-class variations. Since only $(n+1)$ points are required to uniquely determine a polynomial of degree n, this scheme can retrieve the secret K when the number of discrepancies in the biometric data $\left(|X - X'|\right)$ is less than $r - n$. However, this method has a higher computational cost because it requires a large number of polynomial interpolations.

Our fuzzy vault implementation significantly differs from the implementation proposed in [25] in the following aspects.

1) In our implementation, we apply a *minutiae matcher* [26] *during decoding to account for non-linear distortion* in fingerprints where as in [25], the minutia location information is coarsely quantized to compensate for distortion. Since deformation of the fingerprint ridges increases as we move away from the center of the fingerprint area towards the periphery, uniform quantization alone, as used in [25], is not sufficient to handle distortion. The minutiae matcher used in our implementation [26] employs an adaptive bounding box that accounts for distortion more effectively. This is one of the main reasons the proposed approach leads to a significant improvement in the genuine accept rate (GAR).
2) Only the location of minutia points was used for vault encoding in [25]. *We use both minutia location and orientation attributes* which increases the number of chaff points that can be added because we can now add a chaff point whose location is close to a true minutia but with a different direction. Chang et al. [27] have shown that the number of possible chaff points affects the security of the vault. Hence, using both minutia location and orientation makes it more difficult for an attacker to decode the vault. At the same time, when a genuine user is attempting to decode the

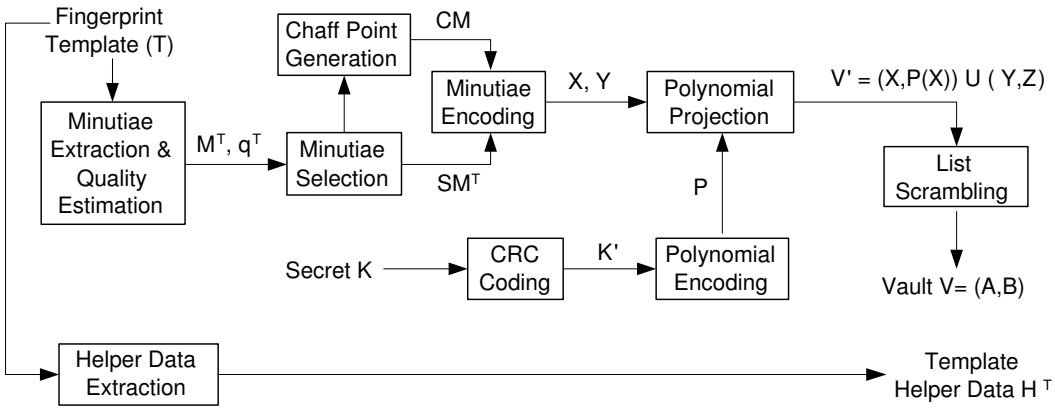

Fig. 4. Proposed implementation of vault encoding.

vault, it is now easier to filter out chaff points from the vault because it is less probable that a chaff point will match with the query minutia in both location and direction. This reduces the decoding complexity by eliminating most of the chaff points from the unlocking set.

3) *We use local image quality index estimated from the fingerprint in order to select the most reliable minutiae* for vault encoding and decoding. This also leads to higher GAR compared to the implementation in [25].
4) Although our alignment technique is similar to the one proposed in [25], *we have made significant changes to the curvature estimation and alignment steps* compared to [25] which results in more accurate alignment between the template and query.

A. Vault Encoding

Figure 4 shows the block diagram of the proposed fuzzy vault encoding scheme. We use the Galois field, $\mathcal{F} = GF(2^{16})$, for constructing the vault. The specific field $GF(2^{16})$ was chosen because it offers a sufficiently *large universe* (number of elements in the field) to ensure vault security [12] and is computationally convenient for the fuzzy vault application. Vault encoding consists of the following eight steps.

1) Given the template fingerprint image T, we first obtain the template minutiae set $M^T = \{m_i^T\}_{i=1}^{N^T}$, where N^T is the number of minutiae in T. The local quality index proposed in [28] is used to estimate the quality of each minutia in T. Let $q\left(m_i^T\right)$ be the quality of the i^{th} minutia and $q^T = \{q\left(m_i^T\right)\}_{i=1}^{N^T}$ be the quality set corresponding to minutiae set M^T. We also extract the helper data set H^T from the template image to be used for alignment during decoding. The details of helper data extraction are presented in Section IV-A.

2) Since only r genuine minutiae points are required to construct the vault, we apply a minutiae selection algorithm to the template minutiae set M^T. This selection algorithm sorts the minutiae based on their quality and sequentially selects the minutiae starting with the highest quality minutia. Moreover, the algorithm selects only well-separated minutiae, i.e., the minimum distance between any two selected minutia points is greater than a threshold δ_1. The distance, D_M, between two minutia points m_i and m_j is defined as

$$D_M(m_i, m_j) = \sqrt{(u_i - u_j)^2 + (v_i - v_j)^2} + \beta_M \Delta(\theta_i, \theta_j), \tag{1}$$

where $\Delta(\theta_i, \theta_j) = \min\left(|\theta_i - \theta_j|, 360 - |\theta_i - \theta_j|\right)$ and β_M is the weight assigned to the orientation attribute (set to 0.2 in our experiments[3]). Selection of well-separated minutiae ensures that they are assigned unique values when they are encoded into the field $\mathcal{F}$. Let $SM^T = \{m_j^T\}_{j=1}^{r}$ denote the selected minutiae set. Note that if the number of minutia points in T is less than r or if the selection algorithm fails to find r well-separated minutiae, we consider it as a failure to capture (FTC) error and no further processing takes place.

[3]Since the variation in the orientation attribute of a minutia point is usually much larger compared to the variation in its location attribute, the orientation difference is assigned a smaller weight than the Euclidean distance between the minutiae locations. The specific value of 0.2 for β_M was determined empirically as a tradeoff between eliminating as many chaff points as possible from the unlocking set while retaining as many genuine points as possible. The above tradeoff also determines the value of the threshold δ_2 used in decoding.

3) The chaff point set $CM = \{m_k\}_{k=1}^{s}$ is generated iteratively as follows. A chaff point $m = (u, v, \theta)$ is randomly chosen such that $u \in \{1, 2, \cdots, U\}$, $v \in \{1, 2, \cdots, V\}$ and $\theta \in \{1, 2, \cdots, 360\}$. The point m is added to CM if the minimum distance (as defined in equation (1)) between m and all points in the set $SM^T \cup CM$ is greater than δ_1.
4) The minutia attributes $u, v,$ and θ are quantized and represented as bit strings of length $\mathcal{B}_u$, $\mathcal{B}_v$ and $\mathcal{B}_\theta$, respectively. If $\mathcal{B}_u$, $\mathcal{B}_v$ and $\mathcal{B}_\theta$ are chosen such that they add up to 16, we can obtain a 16-bit number by concatenating the bit strings corresponding to $u, v,$ and θ. Using this method, minutia points are encoded as elements in the field $\mathcal{F} = GF(2^{16})$. Let $X = \{x_j\}_{j=1}^{r}$ and $Y = \{y_k\}_{k=1}^{s}$ be the encoded values of selected template minutiae and chaff points, respectively, in the field $\mathcal{F}$.
5) Our scheme is designed to secure a secret K of length $16n$ bits, where n is the degree of the encoding polynomial. We append a 16-bit CRC code to secret K to obtain a new secret $K^{'}$ containing $16(n+1)$ bits. The generator polynomial $G(w) = w^{16} + w^{15} + w^2 + 1$ which is commonly known as IBM CRC-16 is used for generating the CRC bits.
6) The secret $K^{'}$ is encoded into a polynomial $\mathcal{P}$ of degree n in $\mathcal{F}$ by partitioning it into $(n+1)$ 16-bit values $c_0, c_1, \cdots, c_n$ and considering them as coefficients of $\mathcal{P}$, i.e., $\mathcal{P}(x) = c_n x^n + \cdots + c_0$.
7) The polynomial $\mathcal{P}$ is evaluated at all the points in the selected minutiae set X to obtain the set $\mathcal{P}(X) = \{\mathcal{P}(x_j)\}_{j=1}^{r}$. The corresponding elements of the sets X and $\mathcal{P}(X)$ form the locking set $L = \{(x_j, \mathcal{P}(x_j))\}_{j=1}^{r}$. A set $Z = \{z_k\}_{k=1}^{s}$ is obtained by randomly selecting values $z_k \in \mathcal{F}$ such that the points (y_k, z_k) do not lie on the polynomial $\mathcal{P}$, i.e, $z_k \neq \mathcal{P}(y_k),\ \forall\ , k = 1, 2, \cdots, s$. The chaff set is defined as $C = \{(y_k, z_k)\}_{k=1}^{s}$. The union of locking and chaff sets is denoted as $V^{'}$.
8) The elements of $V^{'}$ are randomly reordered to obtain the vault V which is represented as $V = \{(a_i, b_i)\}_{i=1}^{t}$, where $t = r + s$. Only the vault V and the helper data H^T are stored in the system.

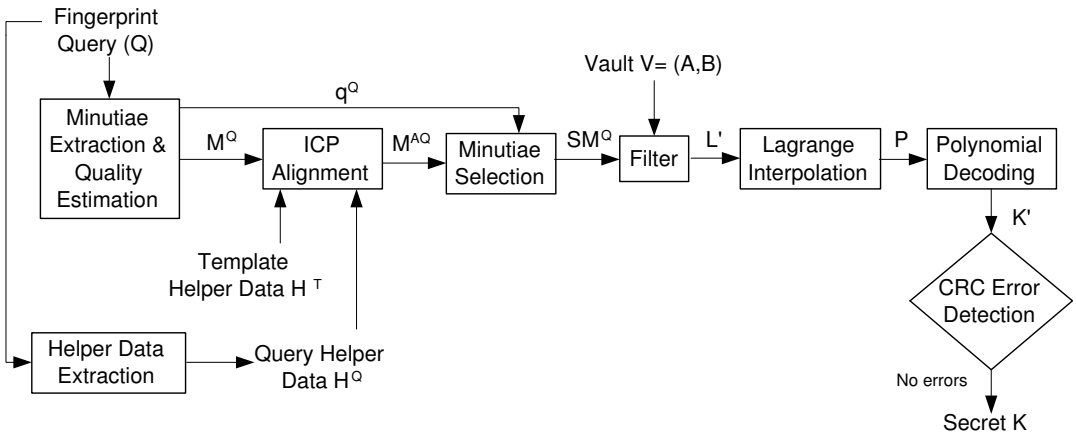

(a)

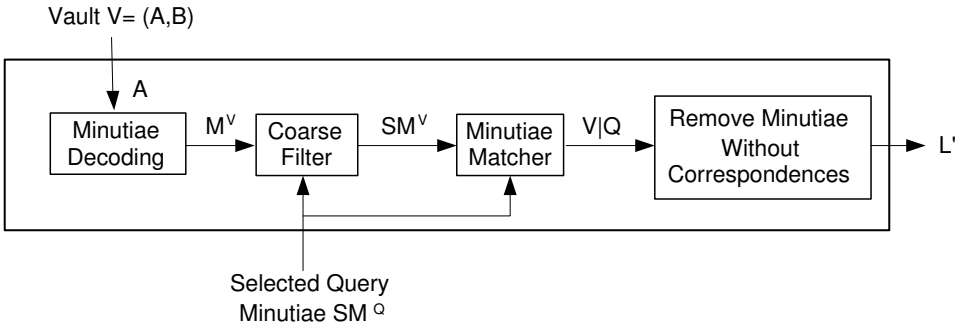

(b)

Fig. 5. Proposed implementation of vault decoding. (a) Block diagram of the complete decoding process and (b) details of the filter used to eliminate the chaff points.

B. Vault Decoding

The process of decoding the vault consists of the following steps (see Figure 5).

1) Given the query fingerprint image Q, we obtain the query minutiae set $M^Q = \{m_i^Q\}_{i=1}^{N^Q}$ and the helper data set H^Q. The quality of each minutia in Q is estimated and the quality set $q^Q = \{q\left(m_i^Q\right)\}_{i=1}^{N^Q}$ corresponding to M^Q is obtained.
2) The alignment algorithm described in Section IV-B is applied and the aligned query minutiae set $M^{AQ} = \{m_i^{AQ}\}_{i=1}^{N^Q}$ is obtained.

3) A minutiae selection algorithm is applied to select r minutiae from the set M^{AQ} based on their quality. The selected minutiae $SM^Q = \{m_j^Q\}_{j=1}^r$ are well-separated in the sense that the minimum distance (as defined in equation (1)) between any two selected minutiae is greater than δ_1. If $N^Q < r$ or if the number of well-separated query minutiae is less than r, it is considered as failure to capture (FTC) and no further processing takes place.

4) The selected query minutiae are used to filter the chaff points in the vault as follows (see Figure 5(b)). The abscissa values of the points in the vault, i.e., $A = \{a_i\}_{i=1}^t$, are first represented as 16-bit strings. The 16-bit strings are partitioned into three strings of lengths $\mathcal{B}_u$, $\mathcal{B}_v$ and $\mathcal{B}_\theta$ which are then converted into quantized minutia attribute values u, v and θ. Thus, we obtain the set $M^V = \{m_i^V = (u_i, v_i, \theta_i)\}_{i=1}^s$.

5) The i^{th} element of the set M^V is marked as a chaff point if the minimum distance between the point $m_i^V \in M^V$ and all the selected minutiae in the query $m_j^Q \in SM^Q$ is greater than a threshold δ_2. We refer to this process as a coarse filter and it filters out a significant proportion of the chaff points (approximately 80%). Let $SM^V = \{m_k^V\}_{k=1}^{N^V}$ be a subset of M^V containing only those elements that are not marked as chaff. Here, N^V is the number of points in M^V that are not marked as chaff and $N^V \ll s$. At this stage, a minutiae matcher [26] is applied to determine the corresponding pairs of minutiae in the sets SM^V and SM^Q. Let $V|Q$ denote the set of correspondences and let $r^{'}$ be the number of correspondences. Since the size of the selected query minutiae set is r, we have $0 \leq r^{'} \leq r$ because each query minutiae can have no more than one corresponding minutia in SM^V. Note that it is also possible to directly apply the minutiae matcher to find correspondences between M^V and SM^Q without any coarse filtering. However, such a method is not effective because the presence of a large number of chaff points in the vault leads to a number of false correspondences. Hence, the coarse filter step is essential before the minutiae matcher is applied.

6) Only those elements of V that are contained in SM^V and which have a corresponding minutia in SM^Q are added to the unlocking set $L^{'}$. The unlocking set is represented as $L^{'} = \{(a_i^{'}, b_i^{'})\}_{i=1}^{r^{'}}$, where $(a_i^{'}, b_i^{'}) = (a_j, b_j)$ if a_j has a corresponding minutia in SM^Q.

7) To find the coefficients of a polynomial of degree n, $(n+1)$ unique projections are necessary. If $r^{'} < (n+1)$, it results in authentication failure. Otherwise, we consider all possible subsets $L^{''}$ of size $(n+1)$ of the unlocking set $L^{'}$ and, for each subset, we construct a polynomial $\mathcal{P}^*$ by Lagrange interpolation. If $L^{''} = \{(a_i^{'}, b_i^{'})\}_{i=1}^{n+1}$ is a specific candidate set, $\mathcal{P}^*(x)$ is obtained as

$$\begin{aligned}\mathcal{P}^*(x) \;=\; & \frac{(x-a_2^{'})(x-a_3^{'})\cdots(x-a_{n+1}^{'})}{(a_1^{'}-a_2^{'})(a_1^{'}-a_3^{'})\cdots(a_1^{'}-a_{n+1}^{'})}\; b_1^{'} + \frac{(x-a_1^{'})(x-a_3^{'})\cdots(x-a_{n+1}^{'})}{(a_2^{'}-a_1^{'})(a_2^{'}-a_3^{'})\cdots(a_2^{'}-a_{n+1}^{'})}\; b_2^{'} \\ & + \cdots + \frac{(x-a_1^{'})(x-a_2^{'})\cdots(x-a_n^{'})}{(a_{n+1}^{'}-a_1^{'})(a_{n+1}^{'}-a_2^{'})\cdots(a_{n+1}^{'}-a_n^{'})}\; b_{n+1}^{'} \end{aligned} \quad (2)$$

The above operations result in a polynomial $\mathcal{P}^*(x) = c_n^* x^n + c_{n-1}^* x^{n-1} + \cdots + c_0^*$.

8) The coefficients $c_0^*, c_1^*, \cdots, c_n^*$ of the polynomial $\mathcal{P}^*$ are 16-bit values which are concatenated to obtain a $16(n+1)$-bit string K^* and CRC error detection is applied to K^*. If an error is detected, it indicates that an incorrect secret has been decoded and we repeat the same procedure for the next candidate set $L^{''}$. If no error is detected, it indicates that $K^* = K^{'}$ with very high probability. In this case, the 16-bit CRC code is removed from K^* and the system outputs the secret K.

IV. Fingerprint Alignment based on Helper Data

The first step in matching two fingerprint images is to align them and determine the area of overlap. Although aligning two fingerprints is a difficult problem in any fingerprint authentication system, it is much more difficult in a biometric cryptosystem like fuzzy vault. This is because the original fingerprint template is not available during authentication and only a transformed version of template is available in the fuzzy vault. Previous implementations of fingerprint-based fuzzy vault either assumed that the template and query fingerprint images are pre-aligned [19] or used a reference point (e.g., core point

[29] or a reference minutia point [20]) for alignment. Though alignment based on a reference point is simple and computationally efficient, it is difficult to determine the reference point reliably and errors in locating the reference point could lead to false rejects. To avoid this problem, we use additional information derived from the fingerprint image, called helper data, to assist in alignment.

Since the helper data is stored as public information, it should not reveal any information about the template minutiae used for constructing the vault because any such leakage would compromise the security. On the other hand, the helper data should carry sufficient information for accurate alignment. Following the approach of Uludag and Jain [25], we extract points of high curvature from the fingerprint orientation field. A trimmed Iterative Closest Point (ICP) algorithm is used to determine the alignment between the template and the query based on this helper data. Since high curvature points are global features in the fingerprint pattern, they do not reveal any information about the minutia attributes which are local characteristics in the fingerprint. Moreover, the helper data does not contain sufficient information to estimate the orientation field or reconstruct the complete fingerprint pattern because the location and curvature values of high curvature points extracted from different classes of fingerprint patterns can be quite similar [30]. Therefore, the proposed helper data does not affect the security of fuzzy vault.

A. Helper Data Extraction

An orientation field flow curve [31] is a set of piecewise linear segments whose tangent direction at each point is parallel to the orientation field direction at that point. Although flow curves are similar to fingerprint ridges, extraction of flow curves is not affected by breaks and discontinuities which are commonly encountered in ridge extraction. Points of maximum curvature in the flow curves along with their curvature values constitute the helper data used in our alignment scheme. Algorithm for extraction of helper data (see Figure 6) consists of four steps: (i) orientation field estimation, (ii) extraction of flow curves, (iii) determination of maximum curvature points and (iv) clustering of high curvature points.

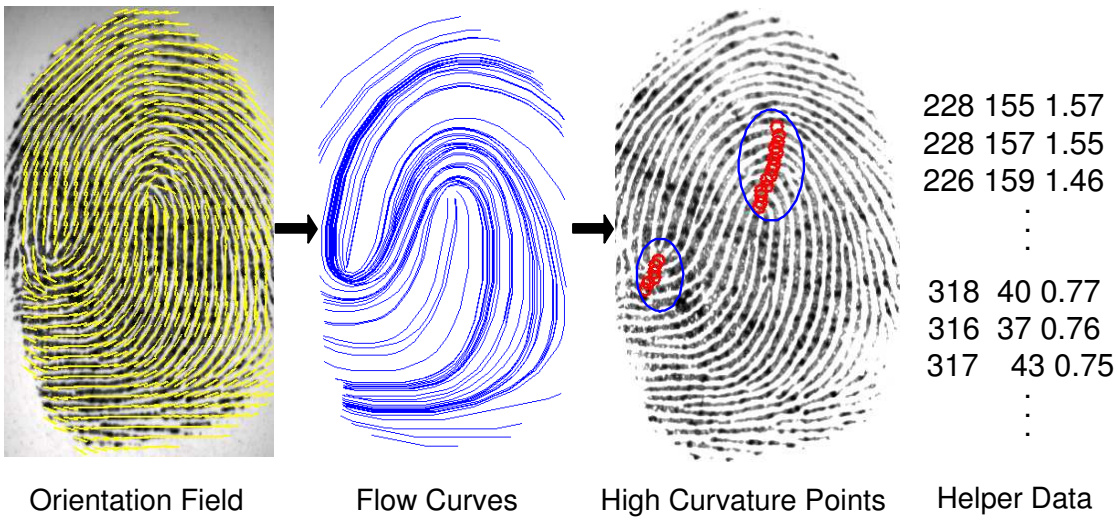

Fig. 6. Algorithm for helper data extraction.

Let $\mathcal{I}$ be a fingerprint image with U rows and V columns. A robust estimate of the orientation field for the given fingerprint image is obtained using the algorithm described in [32]. The flow curve extraction technique described in [31] is used to obtain the set of flow curves based on the estimated orientation field. Each flow curve is represented as a set of points $\{\ell_j\}_{j=1}^{J}$, where J is the number of points in the curve and $\ell_j = (\lambda_j, \mu_j)$ is a point in $\mathcal{I}$, $1 \leq \lambda_j \leq U$ and $1 \leq \mu_j \leq V$, $\forall\ j = 1, 2, \cdots, J$. The sampling interval for the points in a flow curve is set to 5 pixels and the maximum number of samples in a curve is set to 300. Midpoints of the thinned ridges and points in whose neighborhood the orientation field changes significantly are chosen as the starting points for the flow curve extraction.

The curvature (ω) of a point ℓ_j in a flow curve is defined as $\omega_{\ell_j} = 1 - \cos\alpha_{\ell_j}$, where α_{ℓ_j} is the angle between the tangents to the flow curve at the points $\ell_{j-\tau}$ and $\ell_{j+\tau}$, $\forall\ \tau \leq j \leq J - \tau$. The parameter τ is related to the sampling interval of the flow curve and is set to 5. The value of ω_{ℓ_j} is minimum (0) if there is no change in direction as we go from $\ell_{j-\tau}$ to $\ell_{j+\tau}$ through ℓ_j and is maximum (2) if the change in direction is π. The curvature values for the points in the flow curve are estimated and local maxima in the curvature are detected. If the value of the local maximum is greater than σ (set to 0.3), the point

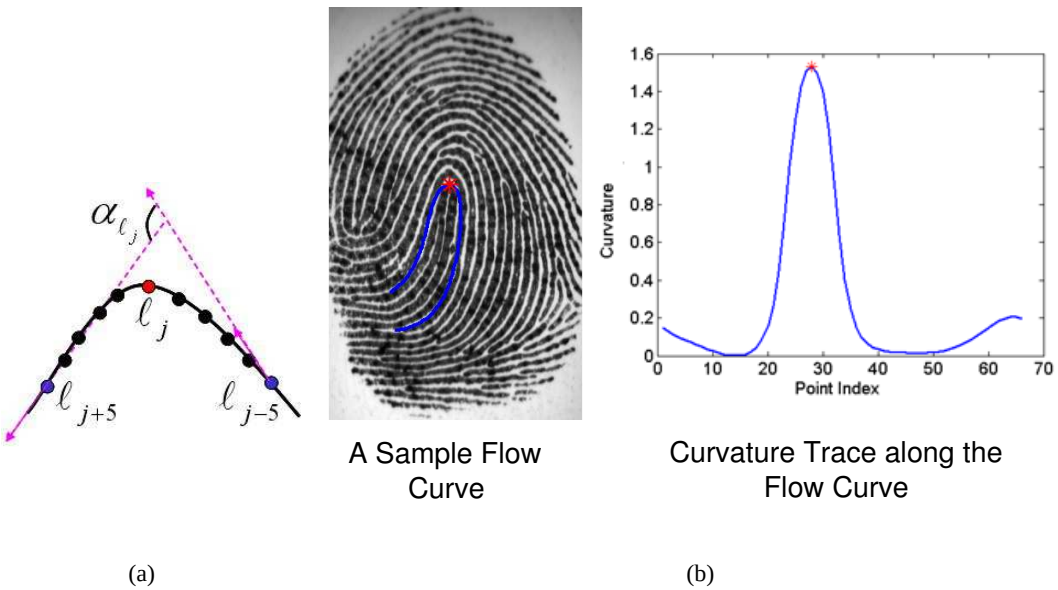

Fig. 7. Determination of maximum curvature points. (a) Curvature estimation at point ℓ_j and (b) trace of curvature for a sample flow curve along with the local maximum.

is marked as a high curvature point and the 3-tuple $h = (\lambda, \mu, \omega)$, where (λ, μ) is the location and ω is the curvature value, is added to the helper data set H. Figure 7 shows the procedure for curvature estimation at a point and a trace of the curvature values for a sample flow curve. Maximum curvature points of all the flow curves are found and the final helper data set is obtained as $H^{\mathcal{I}} = \{h_i\}_{i=1}^{R^{\mathcal{I}}}$, where $R^{\mathcal{I}}$ is the number of helper data points in $\mathcal{I}$. High curvature points tend to occur near the singular points in the fingerprint image. If the image has more than one singularity, points in the helper data set may have many clusters which are identified by applying a single-link clustering algorithm.

B. Alignment using ICP

Let T and Q be the template and query fingerprint images, respectively. Let $H^T = \{h_i^T\}_{i=1}^{R^T}$ and $H^Q = \{h_j^Q\}_{j=1}^{R^Q}$ be the helper data sets obtained from T and Q, respectively. Let $M^Q = \{m_j^Q\}_{j=1}^{N^Q}$ be the query minutiae set, where N^Q is the number of minutia points in Q. We use the Iterative Closest Point (ICP) algorithm proposed by Besl and McKay [33] to align H^T and H^Q and estimate the rigid transformation F. The ICP algorithm starts with two coarsely aligned point sets and iteratively finds the

point correspondences and the rigid transformation between them (for more details see [30]). Since the ICP algorithm strictly assigns a correspondence between every query helper point and a template helper point, there may be alignment errors when the overlap between the two sets is partial. To overcome this problem, we use the trimmed ICP algorithm [34] which ignores a proportion of points in the query set whose distance to the corresponding points in the template set is large. The trimmed ICP algorithm is robust to outliers in the helper data.

Based on the rigid transformation F output by the ICP algorithm, we align the query minutiae set M^Q with the template. Let $M^{AQ} = F\left(M^Q\right) = \{m_j^{AQ}\}_{j=1}^{N^Q}$ represent the query minutiae set after alignment. Figure 8 shows an example of successful minutiae alignment based on helper data and trimmed ICP algorithm. If the number of clusters in H^T and/or H^Q is more than one, the ICP algorithm is repeated for all possible cluster pairs. In this scenario, there will be multiple aligned query minutiae sets. We select the aligned query minutiae set that gives the largest unlocking set $L^{'}$.

V. Experimental Results

The performance of the proposed fuzzy vault implementation has been evaluated on FVC2002-DB2 [35] and MSU-DBI [36] fingerprint databases. The characteristics of these two databases are summarized in Table I. We consider the following three scenarios for vault implementation.

1) One impression is used for encoding and one impression is used for decoding.
2) Two impressions are used for encoding and one impression is used for decoding.
3) Two impressions are used for encoding and two impressions are used for decoding.

When multiple impressions are available for vault encoding, we apply a mosaicing technique [37] to combine the minutiae and helper data from the individual images into a single mosaiced template and helper set. When multiple impressions are available for decoding, we use them sequentially to unlock the vault. The decoding is successful if at least one of the two queries succeeds in unlocking the vault.

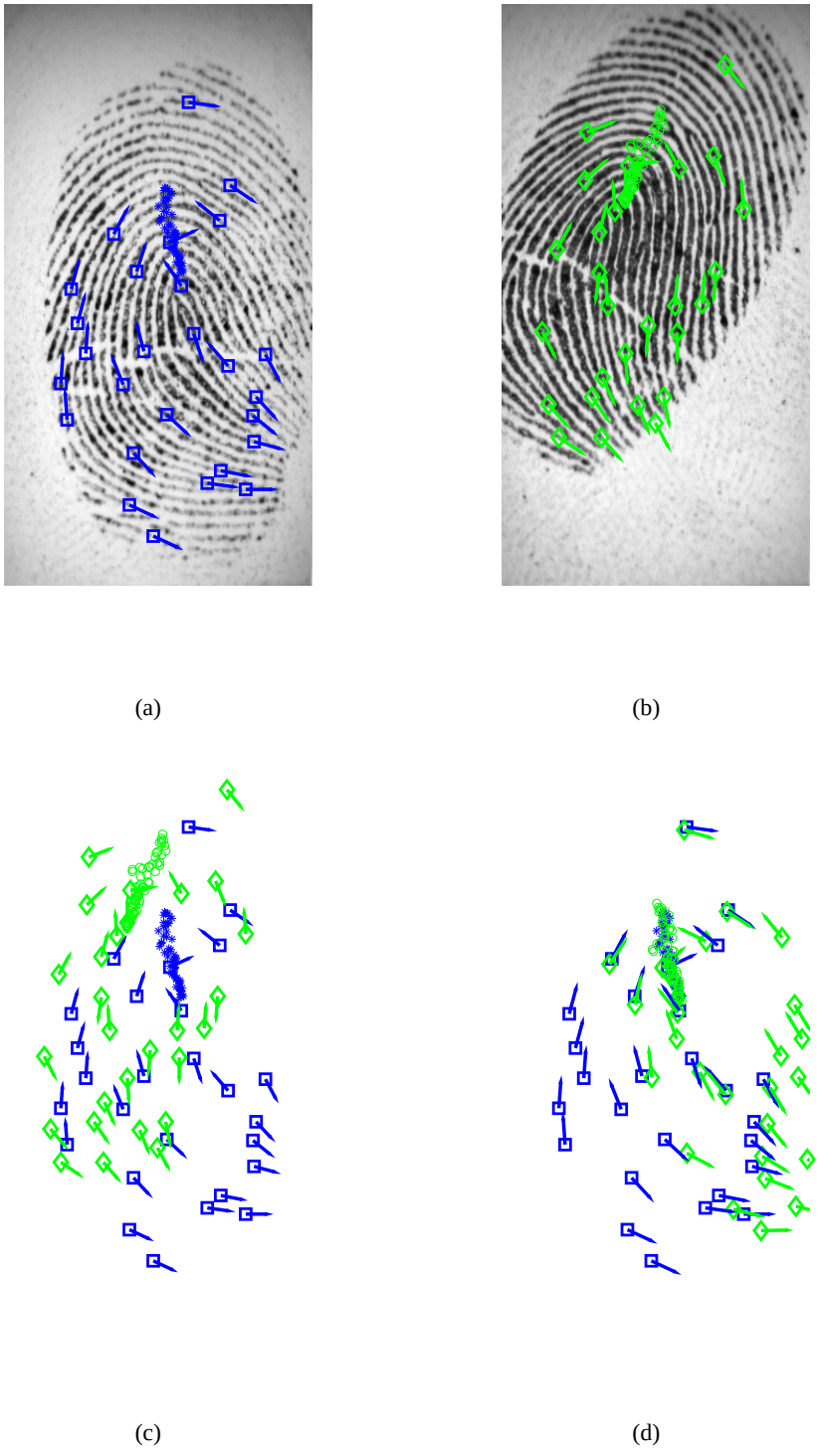

(a) (b)

(c) (d)

Fig. 8. An example of successful minutiae alignment based on helper data and ICP algorithm. (a) Template image with minutiae and helper data, (b) query image with minutiae and helper data (c) template and overlaid query minutiae prior to alignment and (d) template and overlaid query minutiae after alignment. In this figure, the template minutiae are represented as blue squares (tails indicate the minutia direction) and the query minutiae are represented as green diamonds. The template and query helper data points are represented as blue asterisks and green circles, respectively.

TABLE I

SUMMARY OF DATABASES USED IN OUR EXPERIMENTS.

	FVC2002-DB2	**MSU-DBI**
No. of fingers	100	160
No. of impressions/finger	8	4
Sensor	Biometrika FX2000 (Optical)	Digital Biometrics, Inc. (Optical)
Image size	560×296 at 569 dpi resolution	640×480 at 500 dpi resolution
Image quality	Good	Medium

The MSU-DBI database contains two pairs of impressions for each user and these two pairs were collected six weeks apart. Hence, this database is suitable to study the multiple impression scenarios that are considered here. The FVC2002-DB2 database was selected because it is a public-domain database and the images are of relatively good quality. Among the 8 impressions available for each finger in FVC2002-DB2, we use only four impressions (impressions 1, 2, 7 and 8) in our experiments[4].

The parameters used in our implementation for the two databases are listed in Table II. The choice of polynomial degree (n) is related to the size of the secret to be secured. For example, if $n = 8$, we can secure a key of size 128-bits. Since the vault decoding is successful if $(n+1)$ query minutiae match with the template minutiae, the parameter n also affects the error rates. Since the number of minutiae varies for different users, using a fixed value of r (the number of genuine minutiae points in the vault) across all users leads to several failure to capture (FTC) errors. To overcome this problem, we fix the range of r and determine its value individually for each user. The number of chaff points in the vault (s) is chosen

[4]It is quite reasonable to assume that users in a biometric cryptosystem are co-operative and they are willing to provide good quality biometric data in order to retrieve their cryptographic keys. Impressions 3, 4, 5 and 6 in FVC2002 databases were obtained by requesting the users to provide fingerprints with exaggerated displacement and rotation. Hence, these impressions are not representative for the application under consideration. This explains our choice of impressions 1, 2, 7 and 8.

TABLE II

PARAMETERS USED FOR FUZZY VAULT IMPLEMENTATION.

Parameter	**FVC2002-DB2**	**MSU-DBI**
No. of genuine points in the vault, r	18-24	24-36
Degree of encoding polynomial, n	7-10	10-12
Total no. of points in the vault, t	224	336
No. of chaff points in the vault, s	200-206	300-312
Minimum distance between selected minutiae, δ_1	25	25
Maximum distance between a query minutia and points selected by the coarse filter, δ_2	30	40

to be approximately 10 times the number of genuine points in the vault which is a reasonable tradeoff between the complexity of a brute force attack and storage requirements of the vault. The number of bits used for encoding the minutia attributes u, v and θ into the field $\mathcal{F} = GF(2^{16})$ are $\mathcal{B}_u = 6$, $\mathcal{B}_v = 5$ and $\mathcal{B}_\theta = 5$, respectively. The allocation of bits determines the quantization step size for u, v and θ and it depends on the image size. For the selected databases, the above choice was found to be optimal in the sense that the distribution of number of matching minutiae did not change significantly after quantization.

An example of successful vault operation for a user from FVC2002-DB2 when $n = 8$ is shown in Figure 9. Figure 9(f) shows that ICP algorithm leads to correct alignment of query minutiae with the template minutiae concealed in the vault. The coarse filter and minutiae matcher eliminate many chaff points from the vault. The unlocking set mostly consists of genuine points from the vault. For example, in Figure 9(g) we observe that there is only one chaff point in the unlocking set. Since the number of genuine points in the unlocking set is more than 9, the decoding is successful in this example.

The criteria used for evaluating the performance are failure to capture rate (FTCR), genuine accept rate (GAR) and false accept rate (FAR). When the number of well-separated minutiae in the template and/or query fingerprint is less than r, it results in failure to capture. The genuine accept rate is defined

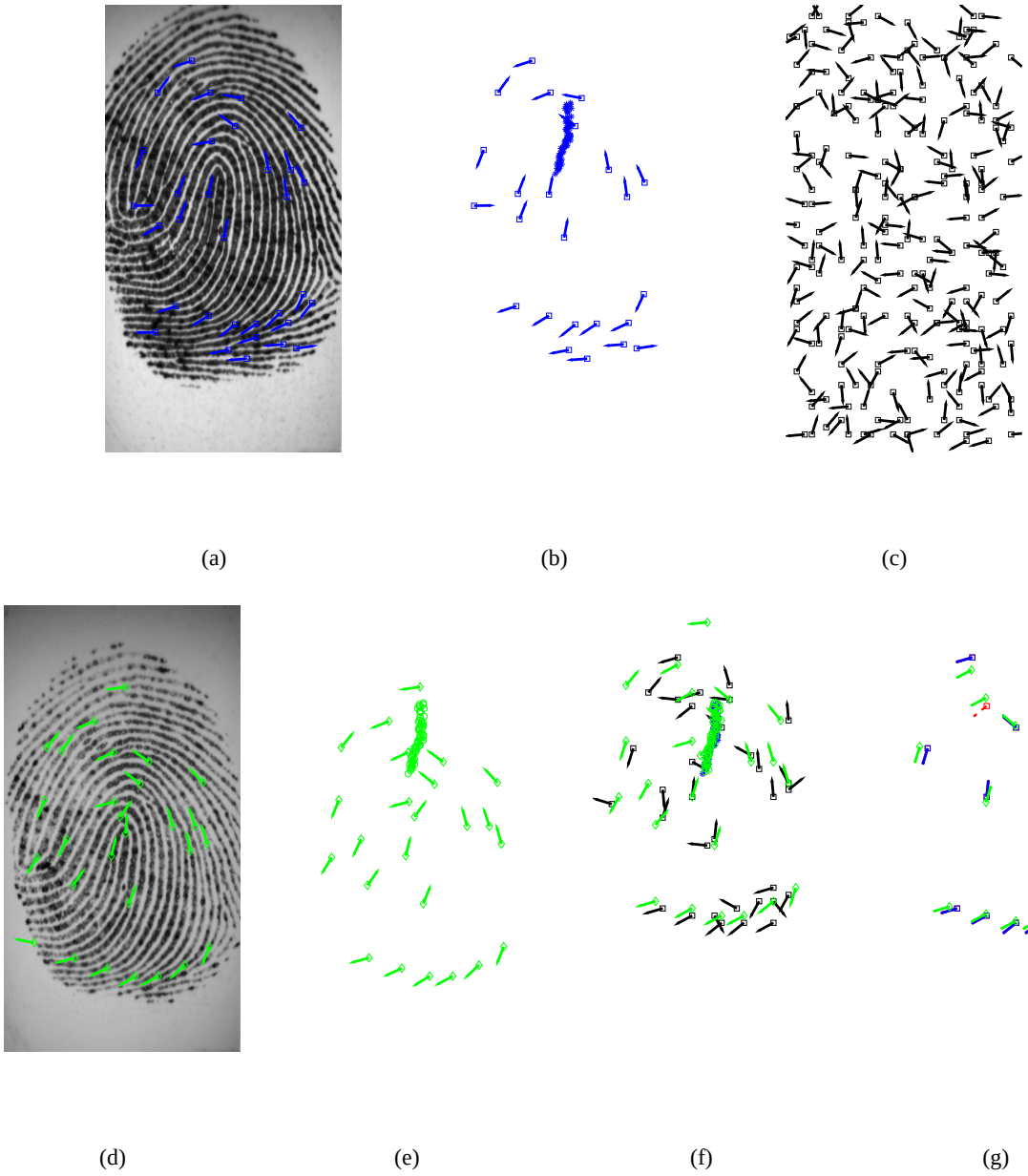

(a) (b) (c)

(d) (e) (f) (g)

Fig. 9. An example of successful operation of the fuzzy vault. (a) Template fingerprint image with minutiae, (b) selected template minutiae and helper data, (c) vault in which the selected template minutiae are hidden among chaff points, (d) query fingerprint image with minutiae, (e) selected query minutiae and helper data, (f) ICP alignment of template and query helper data sets and coarse filtering of chaff points, and (g) unlocking set obtained by applying a minutiae matcher which eliminates almost all the chaff points. The point shown in red in (g) is the only chaff point that remains in the unlocking set. Here, figures (a)-(c) represent vault encoding and (d)-(g) represent decoding.

as the percentage of attempts made by genuine users that resulted in successful authentication. Since a vault is constructed for each finger, the number of genuine attempts is 100 and 160 for the FVC and MSU databases, respectively. The false accept rate is the percentage of attempts made by impostors that resulted in successful decoding of a vault corresponding to a legitimate user. Impostor attempts were simulated by trying to decode a user's vault using impressions from all the other users. The number of impostor attempts is $9,900$ and $25,440$ for the FVC and MSU databases, respectively.

The first row of Table III shows the performance of the proposed vault implementation on the FVC2002-DB2 database for different key sizes when a single impression is used for encoding and decoding (impression 1 is used for encoding and impression 2 for decoding). For example, when the key size is 128 bits ($n = 8$), 91 out of 100 genuine attempts were successful. Among the 9 failed attempts, 2 were due to the lack of sufficient number of minutiae in the template (FTC error). So, only 7 false rejects were actually encountered. For the same experiment, the fuzzy vault implemented in [25] was successful only in 61 out of 100 attempts with a FTCR of 16%. One of the reasons for the high FTCR in [25] is errors in extraction of high curvature points. If the helper data extraction and alignment steps in the implementation of [25] are replaced with the ones proposed in this paper, the FTCR can be reduced to 2% and the GAR can be improved to 74%. This shows that the proposed helper data extraction and alignment algorithms are more robust compared to those presented in [25]. The selection of reliable minutiae based on image quality and use of a minutiae matcher to account for non-linear distortion contribute to further improvement in the GAR from 74% to 91%. The net improvement in the GAR achieved by the proposed implementation over [25] is 30%.

In the case of MSU-DBI database, using a single impression for encoding and decoding results in a higher FTCR of 5.6% and a lower GAR of 82.5% for $n = 11$ (see first row of Table IV). This decrease in performance is due to the lower quality of images in the MSU database compared to FVC2002-DB2. However, the average number of matching minutiae in the MSU database is higher than in FVC2002-DB2

TABLE III

PERFORMANCE SUMMARY OF THE PROPOSED FUZZY VAULT IMPLEMENTATION FOR FVC2002-DB2 DATABASE. HERE, n DENOTES THE DEGREE OF THE ENCODING POLYNOMIAL AND THE MAXIMUM KEY SIZE THAT CAN BE SECURED IS $16n$ BITS.

Scenario	**FTCR (%)**	$n = 7$		$n = 8$		$n = 10$	
		GAR (%)	**FAR (%)**	**GAR (%)**	**FAR (%)**	**GAR (%)**	**FAR (%)**
1 Template, 1 Query	2	91	0.13	91	0.01	86	0
Mosaiced Template, 1 Query	1	95	0.12	94	0.02	88	0
Mosaiced Template, 2 Queries	1	97	0.24	96	0.04	90	0

TABLE IV

PERFORMANCE SUMMARY OF THE PROPOSED FUZZY VAULT IMPLEMENTATION FOR MSU-DBI DATABASE.

Scenario	**FTCR (%)**	$n = 10$		$n = 11$		$n = 12$	
		GAR (%)	**FAR (%)**	**GAR (%)**	**FAR (%)**	**GAR (%)**	**FAR (%)**
1 Template, 1 Query	5.6	85	0.08	82.5	0.02	78.8	0
Mosaiced Template, 1 Query	2.5	88.1	0.09	83.1	0.02	81.2	0
Mosaiced Template, 2 Queries	0	96.9	0.16	92.5	0.03	87.5	0

which allows us to accommodate a larger key size.

The proposed alignment technique based on high curvature points also performs better than registration based on core point. Since it is difficult to determine the core point reliably, alignment based on core points leads to larger false rejects and failure to capture errors. For example, when core point based alignment[5] is used (instead of high curvature points) in the proposed vault implementation, the FTCR increases from 2% to 6% in the FVC database and from 5.6% to 15.6% in the MSU database. The reasons for increase in FTCR are (i) no core point is present in some of the images (e.g., arch fingerprints) and (ii) the algorithm fails to find the core point in some images (e.g., images where the loops are not very

[5]The core point was detected using a commercial-off-the-shelf fingerprint recognition software from Neurotechnologija.

prominent). These are well-known problem in core point detection. Furthermore, errors in finding the exact location and direction of the core point leads to a reduction in the GAR. The GAR decreases from 91% to 81% ($n = 8$) and from 82.5% to 77.5% ($n = 11$) in the FVC and MSU databases, respectively. These results clearly demonstrate the merits of using alignment based on high curvature points compared to core-based alignment.

One way to improve the performance of the vault is to use multiple impressions (templates) from the same finger during enrollment. However, we cannot create a vault for each enrolled image because an attacker can compare the multiple vaults and identify the chaff points. Therefore, we obtain a single mosaiced template from two impressions and use the mosaiced minutiae to construct the vault. From row 2 of Table III we observe that mosaicing reduces the FTCR from 2% to 1% and also increases the GAR of the system for all values of n. The performance can be further improved by using multiple queries during authentication. In case of 128-bit key size ($n = 8$) for FVC2002-DB2 database, mosaiced template leads to a GAR of 94% and using two queries instead of one query increases the GAR to 96%. The use of multiple impressions also leads to significant reduction of FTCR and increase in GAR for the MSU-DBI database (see rows 2 and 3 of Table IV).

The false rejects in our experiments were either due to errors in helper data extraction or due to insufficient number of matching minutiae in the overlapping region between the template and query. Figure 10 shows an example where the false reject is due to incorrect helper data extraction. In this case, the helper data for template fingerprint is inaccurate because the region of high curvature (core region) is close to the image boundary (see Figure 10(a)). An example of failure due to insufficient number of overlapping minutiae is presented in Figure 11. While the alignment between the template and query images in Figure 11 is accurate, there are only 5 matching minutiae. This leads to a false reject because at least 9 genuine minutiae must be identified in the vault for successful decoding.

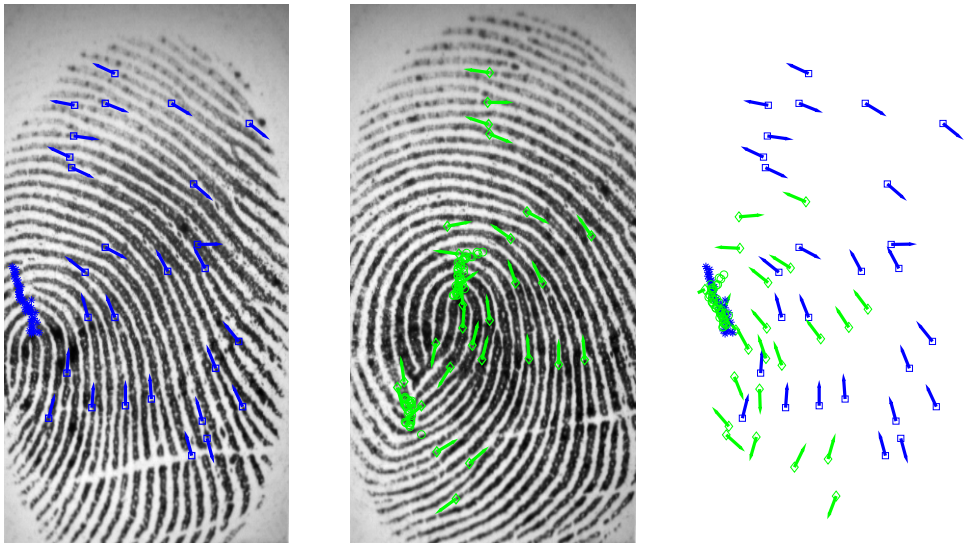

(a) (b) (c)

Fig. 10. Failure due to incorrect helper data extraction. (a) Template fingerprint image with minutiae and helper data, (b) query fingerprint image with minutiae and helper data, and (c) ICP alignment of template and query helper data sets along with aligned template and query minutiae. Helper data is incorrect in the template because the high curvature region is near the boundary.

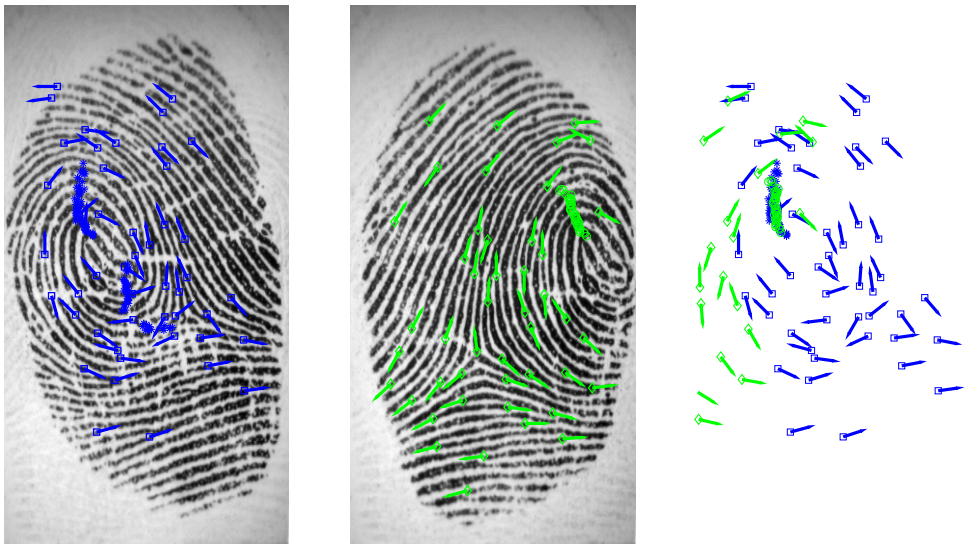

(a) (b) (c)

Fig. 11. Failure due to partial overlap. (a) Template fingerprint image with minutiae and helper data, (b) query fingerprint image with minutiae and helper data, and (c) ICP alignment of template and query helper data sets along with aligned template and query minutiae. Though the alignment is accurate, there are only few matching minutiae in these two images.

The FAR of the proposed fuzzy vault implementation is non-zero for smaller values of n. In the single impression scenario for FVC2002-DB2, when $n = 8$, we observed one false accept in $9,900$ impostor attempts. The template and query fingerprint pair which gives rise to a false accept is shown in Figure 12. Analysis of this false accept example indicates that there is indeed a set of 9 minutiae in the query which matches with the template minutiae in both location and direction (see Figure 12(c)). Since the vault decoding is successful if $(n+1)$ points in the query minutiae set (of size r) match with the template minutiae, the genuine accept and false accept rates vary with n when r is fixed. Reducing n increases both GAR and FAR and increasing n lowers both GAR and FAR. As observed from Table III, FAR is high when $n = 7$ and is zero when $n = 10$. We also observe a marginal decrease in the GAR when n is increased from 7 to 10. The FAR for the MSU-DBI database also shows a similar behavior.

As pointed out earlier, a drawback of the modified fuzzy vault scheme in [24] compared to the original scheme in [7] is the need to verify multiple candidate secrets. In [24] it was reported that an average of 201 candidate secrets were evaluated corresponding to 52 seconds of computation in Matlab with a 3.4 GHz processor system. In our implementation, the use of minutiae orientation in addition to the location eliminates almost all the chaff points from the unlocking set. Therefore, the median number of candidate secrets that need to be evaluated is only 2 (mean is 33) and the median decoding time is 3 seconds (mean is 8 seconds) on a similar processor.

VI. Security of Proposed Fuzzy Vault Implementation

The security provided by the fuzzy vault scheme has been studied theoretically in [7], [12], [27]. Here, we consider three possible ways in which the proposed fingerprint-based fuzzy vault implementation can be circumvented in practice. Suppose an attacker attempts a brute-force attack on the proposed system by trying to decode the secret using all combinations of $(n + 1)$ points in the vault. If the secret size is 128 bits and the number of genuine and chaff points in the vault are 24 and 200, respectively, the total

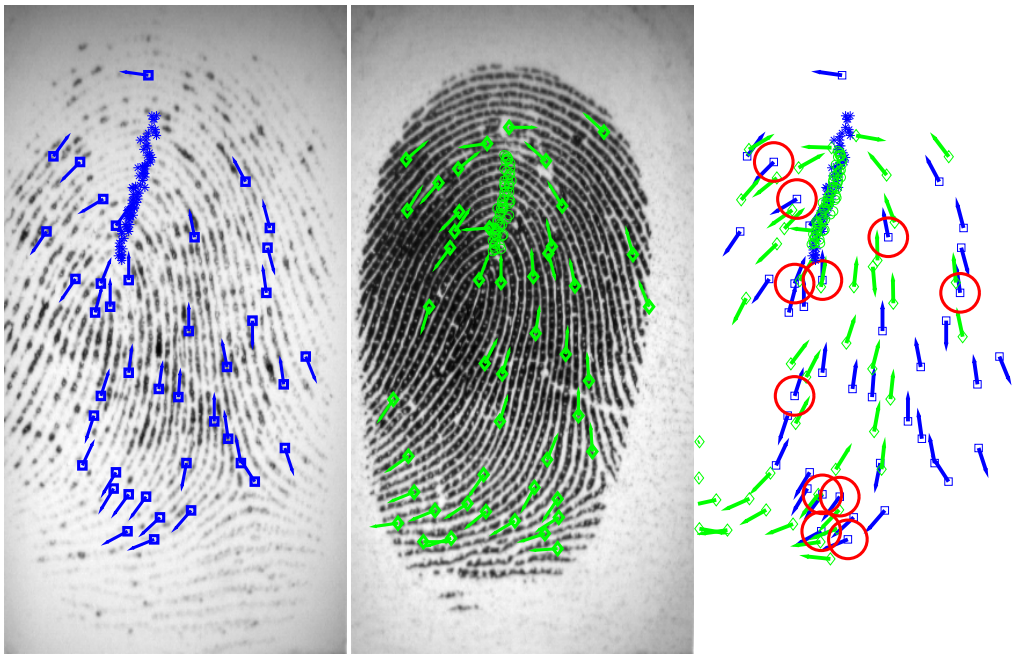

(a) (b) (c)

Fig. 12. An example of false accept when $n = 8$. (a) Template fingerprint image with minutiae and helper data, (b) query fingerprint image with minutiae and helper data, and (c) ICP alignment of template and query helper data sets along with aligned template and query minutiae. In (c), we observe that there are 9 matching minutiae between the query and the template.

number of possible combinations is $\binom{224}{9} \approx 3.3 \times 10^{15}$ and among these combinations $\binom{24}{9} \approx 1.3 \times 10^{6}$ combinations will successfully decode the secret. The probability that a combination of points decodes the secret is $\frac{1.3\times10^{6}}{3.3\times10^{15}} \approx 4 \times 10^{-10}$ and the expected number of combinations that need to be evaluated is 2.5×10^{9}. This corresponds to a computational time of 13 years based on our current implementation.

The second method of circumvention involves the extraction of information from the helper data. We have already pointed out that high curvature points do not reveal any information about the minutiae and it is not possible to estimate the orientation field using only the high curvature points. However, suppose a smart attacker is able to extract the orientation field from the helper data and uses it to identify the chaff points. We can still defend against such an attack by adding sufficient number of chaff points that

are consistent with the orientation field (i.e., the location of the chaff minutia is random, but its direction is determined by the orientation field) in addition to the completely random chaff points.

In our implementation, we assume that the spatial distribution of minutiae in a fingerprint image is uniform and use this property in the generation of chaff points. However, this assumption is not true because minutiae often tend to occur in clusters. Hence, the attacker may use statistical models for the minutiae distribution to classify the points in the vault as genuine and chaff and attempt a brute-force attack using only the perceived genuine points. One way to defend against such attacks is to use statistical distribution of minutiae for the generation of chaff points during vault construction. Another solution is to use alternate fuzzy constructions that avoid the need for chaff points, such as the one proposed in [12]. However, such schemes usually require more robust techniques for alignment and non-linear distortion correction and their implementation based on fingerprint minutiae does not appear to be practical.

VII. Summary and Future Work

Given the rising magnitude of identity theft in our society, it is imperative to have reliable security mechanisms to protect information systems. Although cryptography is a powerful tool to achieve information security, the security of cryptosystems relies on the fact that cryptographic keys are secret and known only to the legitimate user. Biometric systems are being widely used to achieve reliable user authentication and these systems will proliferate into the core information infrastructure of the (near) future. When this happens, it is crucial that biometric authentication is secure. Fuzzy vault is one of the most comprehensive mechanisms for secure biometric authentication and cryptographic key protection. We have implemented a *fully automatic* and *practical* fuzzy vault system based on fingerprint minutiae that can easily secure secrets such as 128-bit AES encryption keys. The main challenge in the implementation of a fingerprint-based fuzzy vault is the alignment of the query with the transformed template stored in the vault. We use helper data derived from the orientation field to align the template and query minutiae sets

without leaking any information about the minutiae. Moreover, we have shown that applying a minutiae matcher during decoding can effectively compensate for non-linear distortion resulting in a significant improvement in the genuine accept rate. Evaluation on a *public-domain fingerprint database* demonstrates that our implementation has the *highest genuine accept rate* and a very low false accept rate among the known implementations of fingerprint-based fuzzy vault.

The performance of the fuzzy vault can be further improved by using multiple biometric sources such as multiple fingers or multiple modalities (e.g., fingerprint and iris). Apart from the location and orientation attributes of a minutia point, many minutiae-based fingerprint matchers use additional attributes like minutia type, ridge counts, ridge curvature and ridge density to achieve high recognition rates. These attributes could also be incorporated into the fuzzy vault framework. Addition of new attributes will not only increase the number of possible chaff points that can added to the vault but also decrease the decoding complexity for genuine users and reduce the false accept rate. A well-known limitation of the fuzzy vault framework is its dependence on chaff points to achieve security. Therefore, fuzzy constructions that do not involve chaff points could be considered.

REFERENCES

[1] W. Stallings, *Cryptography and Network Security: Principles and Practices*. Prentice Hall, 2006.

[2] RSA Laboratories, "PKCS #5: Password-Based Crptography Standard, Version 2.0," RSA, Tech. Rep., March 1999.

[3] K. Mitnick, W. Simon, and S. Wozniak, *The Art of Deception: Controlling the Human Element of Security*. Wiley, 2002.

[4] A. K. Jain, A. Ross, and S. Prabhakar, "An Introduction to Biometric Recognition," *IEEE Transactions on Circuits and Systems for Video Technology*, vol. 14, no. 1, pp. 4–20, January 2004.

[5] N. K. Ratha, J. H. Connell, and R. M. Bolle, "An Analysis of Minutiae Matching Strength," in *Proceedings of Audio- and Video-based Biometric Person Authentication*, Halmstad, Sweden, June 2001, pp. 223–228.

[6] D. Maltoni, D. Maio, A. K. Jain, and S. Prabhakar, *Handbook of Fingerprint Recognition*. Springer-Verlag, 2003.

[7] A. Juels and M. Sudan, "A Fuzzy Vault Scheme," in *Proceedings of IEEE International Symposium on Information Theory*, Lausanne, Switzerland, 2002, p. 408.

[8] G. I. Davida, Y. Frankel, and B. J. Matt, "On Enabling Secure Applications Through Off-Line Biometric Identification," in *Proceedings of IEEE Symposium on Security and Privacy*, Oakland, USA, May 1998, pp. 148–157.

[9] C. Soutar, D. Roberge, A. Stoianov, R. Gilroy, and B. V. K. V. Kumar, "Biometric Encrpytion," in *ICSA Guide to Cryptography*, R. K. Nichols, Ed. McGraw Hill, 1999.

[10] F. Monrose, M. Reiter, Q. Li, and S. Wetzel, "Cryptographic Key Generation from Voice," in *Proceedings of IEEE Symposium on Security and Privacy*, Oakland, USA, May 2001, pp. 202–213.

[11] A. Juels and M. Wattenberg, "A Fuzzy Commitment Scheme," in *Proceedings of Sixth ACM Conference on Computer and Communications Security*, Singapore, November 1999, pp. 28–36.

[12] Y. Dodis, R. Ostrovsky, L. Reyzin, and A. Smith, "Fuzzy Extractors: How to Generate Strong Keys from Biometrics and Other Noisy Data," Cryptology ePrint Archive, Tech. Rep. 235, February 2006.

[13] F. Hao, R. Anderson, and J. Daugman, "Combining Crypto with Biometrics Effectively," *IEEE Transactions on Computers*, vol. 55, no. 9, pp. 1081–1088, September 2006.

[14] P. Tuyls, A. H. M. Akkermans, T. A. M. Kevenaar, G.-J. Schrijen, A. M. Bazen, and R. N. J. Veldhuis, "Practical Biometric Authentication with Template Protection," in *Proceedings of AVBPA*, Rye Town, USA, July 2005, pp. 436–446.

[15] E. Martinian, S. Yekhanin, and J. Yedidia, "Secure Biometrics Via Syndromes," Mitsubishi Electric Research Laboratories, Tech. Rep. TR2005-112, December 2005.

[16] N. K. Ratha, J. H. Connell, and R. M. Bolle, "Enhancing Security and Privacy in Biometric Authentication Systems ," *IBM Systems Journal*, vol. 40, no. 3, pp. 614–634, 2001.

[17] U. Uludag, S. Pankanti, S. Prabhakar, and A. K. Jain, "Biometric Cryptosystems: Issues and Challenges," *Proceedings of the IEEE, Special Issue on Multimedia Security for Digital Rights Management*, vol. 92, no. 6, pp. 948–960, June 2004.

[18] E. R. Berlekamp, *Algebraic Coding Theory*. McGraw Hill, 1968.

[19] T. Clancy, D. Lin, and N. Kiyavash, "Secure Smartcard-Based Fingerprint Authentication," in *Proceedings of ACM SIGMM Workshop on Biometric Methods and Applications*, Berkley, USA, November 2003, pp. 45–52.

[20] S. Yang and I. Verbauwhede, "Automatic Secure Fingerprint Verification System Based on Fuzzy Vault Scheme," in *Proceedings of IEEE ICASSP*, vol. 5, Philadelphia, USA, March 2005, pp. 609–612.

[21] Y. Chung, D. Moon, S. Lee, S. Jung, T. Kim, and D. Ahn, "Automatic Alignment of Fingerprint Features for Fuzzy Fingerprint Vault," in *Proc. of Conf. on Information Security and Cryptology*, Beijing, China, Dec. 2005, pp. 358–369.

[22] Y. C. Feng and P. C. Yuen, "Protecting Face Biometric Data on Smartcard with Reed-Solomon Code," in *Proceedings of CVPR Workshop on Privacy Research In Vision*, New York, USA, June 2006, p. 29.

[23] M. Freire-Santos, J. Fierrez-Aguilar, and J. Ortega-Garcia, "Cryptographic Key Generation Using Handwritten Signature,"

in *Proceedings of Biometric Technologies for Human Identification III*, vol. 6202, Orlando, USA, April 2006, pp. 225–231.

[24] U. Uludag, S. Pankanti, and A. K. Jain, "Fuzzy Vault for Fingerprints," in *Proceedings of Audio- and Video-based Biometric Person Authentication*, Rye Town, USA, July 2005, pp. 310–319.

[25] U. Uludag and A. K. Jain, "Securing Fingerprint Template: Fuzzy Vault With Helper Data," in *Proceedings of CVPR Workshop on Privacy Research In Vision*, New York, USA, June 2006, p. 163.

[26] A. K. Jain, L. Hong, and R. Bolle, "On-line Fingerprint Verification," *IEEE Transactions on Pattern Analysis and Machine Intelligence*, vol. 19, no. 4, pp. 302–314, April 1997.

[27] E.-C. Chang, R. Shen, and F. W. Teo, "Finding the Original Point Set Hidden Among Chaff," in *Proceedings of ACM Symposium on Information, Computer and Communications Security*, Taipei, Taiwan, 2006, pp. 182–188.

[28] Y. Chen, S. C. Dass, and A. K. Jain, "Fingerprint Quality Indices for Predicting Authentication Performance," in *Proceedings of AVBPA*, Rye Brook, USA, July 2005, pp. 160–170.

[29] N. K. Ratha, S. Chikkerur, J. H. Connell, and R. M. Bolle, "Generating Cancelable Fingerprint Templates," *IEEE Transactions on Pattern Analysis and Machine Intelligence*, vol. 29, no. 4, pp. 561–572, April 2007.

[30] K. Nandakumar, A. K. Jain, and S. Pankanti, "Fingerprint-based Fuzzy Vault: Implementation and Performance," Michigan State University, Tech. Rep. TR-06-31, 2006, Available at http://www.cse.msu.edu/cgi-user/web/tech/document?ID=675.

[31] S. C. Dass and A. K. Jain, "Fingerprint Classification Using Orientation Field Flow Curves," in *Proceedings of Indian Conference on Computer Vision, Graphics and Image Processing*, Kolkata, India, December 2004, pp. 650–655.

[32] S. C. Dass, "Markov Random Field Models for Directional Field and Singularity Extraction in Fingerprint Images," *IEEE Transactions on Image Processing*, vol. 13, no. 10, pp. 1358–1367, October 2004.

[33] P. Besl and N. McKay, "A Method for Registration of 3-D Shapes," *IEEE Transactions on Pattern Analysis and Machine Intelligence*, vol. 14, no. 2, pp. 239–256, February 1992.

[34] D. Chetverikov, D. Svirko, D. Stepanov, and P. Krsek, "The Trimmed Iterative Closest Point Algorithm," in *Proceedings of International Conference on Pattern Recognition*, Quebec City, Canada, August 2002, pp. 545–548.

[35] D. Maio, D. Maltoni, J. L. Wayman, and A. K. Jain, "FVC2002: Second Fingerprint Verification Competition," in *Proceedings of International Conference on Pattern Recognition*, Quebec City, Canada, August 2002, pp. 811–814.

[36] A. K. Jain, S. Prabhakar, and A. Ross, "Fingerprint Matching: Data Acquisition and Performance Evaluation," Michigan State University, Tech. Rep. TR99-14, 1999.

[37] A. Ross, S. Shah, and J. Shah, "Image Versus Feature Mosaicing: A Case Study in Fingerprints," in *Proceedings of SPIE Conference on Biometric Technology for Human Identification*, vol. 6202, Orlando, USA, April 2006, pp. 1–12.